

CleanAtlantic

Tackling Marine Litter in the Atlantic Area

Integration of UAS surveys in marine litter monitoring of coastal and remote areas

WP 5: Mapping litter distribution for clean-ups

Activity 2: Monitoring the presence of ML in the Marine Environment

WP	5 – MAPPING LITTER DISTRIBUTION FOR CLEAN-UPS
ACTION	5. 2 – MONITORING THE PRESENCE OF ML IN THE MARINE ENVIRONMENT
LAST UPDATE	09/08/2023
VERSION	1
AUTHORS	JOÃO G. MONTEIRO ARDITI/MARE-Madeira SILVIA ALMEIDA ARDITI/MARE-Madeira MARISA GOUVEIA ARDITI/MARE-Madeira SOLEDAD ÁLVAREZ ARDITI/MARE-Madeira NICOLA PESTANA DRAAC PEDRO SEPÚLVEDA DRAAC/MARE-Madeira JOÃO CANNING-CLODE ARDITI/MARE-Madeira
PARTICIPANTS	ARDITI, DRAAC

DISCLAIMER

This document covers activities implemented with the financial assistance of the INTERREG Atlantic Area. It only reflects the author's view, thus the Atlantic Area Programme authorities are not liable for any use that may be made of the information contained therein.

INDEX

INTEGRATION OF UAS SURVEYS IN MARINE LITTER MONITORING OF COASTAL AND REMOTE AREAS

1. INTRODUCTION	4
2. MATERIALS AND METHODS	6
2.1. In situ litter surveys	6
2.2. MARE-Madeira/ARDITI	7
2.3. Accumulation detection	7
2.4. Mapping beached litter concentration	9
3. RESULTS	10
3.1. Accumulation detection	10
3.2. Mapping beached litter concentration	10
4. DISCUSSION	14
5. CONCLUSION	16
6. REFERENCES	17
ANNEX I –	18
ANNEX II –	29

Integration of UAS surveys in marine litter monitoring of coastal and remote areas

1. INTRODUCTION

This study is a follow up of the first stage of CleanAtlantic project and assesses the integration of aerial surveys from Unmanned Aerial Systems (UAS) to monitor marine litter in coastal areas and remote locations.

To great extent, many of the efforts and advances in dealing with marine litter pollution are still focused in “diagnosing” the problem, including: establishing protocols to detect, monitor and characterise marine litter distribution, identify major sources and assess the multiple impacts of the various types of marine litter. Similarly to other locations across the globe, monitoring initiatives in Europe and in the Atlantic area face numerous challenges and difficulties in regularly collecting data in such an extremely dynamic, complex and three dimensional environment like the marine realm. This has likely contributed to most efforts by well-established monitoring programs and dedicated survey protocols to target Beached litter.

This case study was designed to complement DRAAC ongoing marine litter monitoring program in Madeira, which currently covers 10 beaches in Madeira and Porto Santo islands, following the OSPAR beach litter monitoring protocol and within the scope of the Marine Strategy Framework Directive Monitoring Programs.

While OSPAR and other in situ detailed survey protocols are widely used to assess litter pollution and characterize marine litter, they are typically limited to a relatively small section of the shoreline (e.g. 100 meter transects). This approach enables a very detailed characterization of the marine litter, which is essential to better understand which type of litter is more concerning and to design policies and measures to mitigate the problem. However, these protocols generally fail to assess how litter is distributed beyond the 100 meters surveyed, meaning they do not provide information on litter pollution and concentrations along the shorelines or beaches. In addition, remote locations that are not easily accessible for in situ surveys are generally overlooked by surveys and clean-ups.

The use of UAS surveys combined with structure from motion photogrammetry, imagery analysis and Artificial Intelligence (AI) has been pushed forward over the last 5 years (1), illustrating how technological advances in commercially available drones and analytical processes have been evolving. However, most of these advances have been constrained to the academia and research, as most of them are widely disseminated and made available for the public and for authorities to leverage. With a wide range of UAS systems available, this constrain is mostly due to limitations in imagery processing (1, 2). Commercial of the shelf drones with programmable flight paths and with image sensors can easily be acquired at reasonable cost, but the software and computational infrastructure required to create photomosaics for analysis is often expensive and tools to leverage Deep Learning and Artificial Intelligence still require computation skills and training (1-5). Additionally, AI and deep learning tools for object detection and litter classification have a

classification tree and labels that don't meet the level of detail required for International and European monitoring reporting (e.g. OSPAR and MSFD,).

With this perspective, this case study focused in assessing the use of UAS remote sensing and tested a workflow that can be easily implemented and upscaled by authorities, managers, NGOs and other stakeholders. The goal was to provide a guideline and suggestions for easy integration of UAS surveys independently or to complement in situ monitoring and sampling that can be used to map marine litter concentration in remote areas and/or in wider areas beyond the in situ sampling area. Parameters for the test were: i) the drone needed to be readily available for purchase for a value under 2000€; ii) flight operations need to be automated; iii) mosaic reconstruction and litter item detection and mapping can not rely on programming and/or advanced IT skills or resources, and; iv) the final product needs to provide spatially explicit data on litter concentration.

2. MATERIALS AND METHODS

2.1. In situ litter surveys:

For the purposes of this study, research activities and tests focused on beaches and coastal areas where the DRAAC is monitoring marine litter (Table 1). A total of 10 beaches are currently being monitored by DRAAC staff using the OSPAR protocol. First implemented in the fall of 2020, a total of 72 surveys have been conducted to date.

Data from these surveys were inspected and sorted to be used within the scope of this case study, to characterize and as references for litter pollution in a select set of locations.

Table 1. List of OSPAR regular monitoring beaches, dates and survey numbers.

OSPAR ID	Type of monitoring	Last OSPAR Period	Year	Beach	Date	Survey number	Date of first survey
26	Regular	Winter	2023	Vila - São Vicente	3-Feb-23	7	Fall 2020
27	Regular	Winter	2023	Galé - Calheta	11-Jan-23	10	Fall 2020
28	Regular	Winter	2023	Fajã dos Padres	20-Jan-23	10	Fall 2020
29	Regular	Winter	2023	Praia do Gastão - Porto Santo	18-Jan-23	9	Fall 2020
30	Regular	Winter	2023	Maiata - Porto da Cruz	24-Jan-23	8	Spring 2021
31	Regular	Winter	2023	Calhau da Serra de Dentro	19-Jan-23	7	Summer 2021
32	Regular	Winter	2023	Arsenal - Portinho	12-Jan-23	7	Summer 2021
33	Regular	Winter	2023	Calhau das Achadas da Cruz	26-Jan-23	5	Winter 2022
34	Regular	Winter	2023	Baía d'Abra - Caniçal	27-Jan-23	5	Winter 2022
35	Regular	Winter	2023	Água d' Alto - São Vicente	23-Jan-23	4	Spring 2022

2.2. MARE-Madeira/ARDITI

For the purposes of this study, ARDITI/MARE-Madeira team planned to conduct UAS surveys in different beaches and with different flight parameters to assess, test and optimize operations and design a streamlined survey workflow that could be used to: i) detect litter in remote locations, and; ii) to complement DRAAC's team in situ surveys to map litter concentration in areas beyond the *in situ* sampling.

Flights were constrained to areas where drone flight operations are possible and by weather. All possible flight operations were coordinated to be prior and in tandem with DRAAC survey and sampling (i.e. when possible in the same day, if not a maximum of 1-2 days before *in situ* monitoring).

A total of ten flights were conducted (Table 2) under different circumstances and with different flight parameters in order to test and develop the operational guidelines: eight flights for mapping and two flights to detect litter accumulations in remote locations and direct clean-up efforts.

Aerial surveys used a DJI Mavic 2 ZOOM, a widely available quadcopter with a 1" CMOS with 20 million effective pixels and a 77° pf maximum field of view. Flight operations relied on DJI Groundstation iOS software installed in an iPad connected to a DJI MAVIC remote controller.

Table 2. List of UAS survey flights for.

Site/Beach	Date	Flights	Altitude (m)	Area (m2)	Flight objective	Images collected
Calheta	2022-09-23	1	30	3,165.50	ML mapping	127
		1	100	19,535.03	ML mapping	96
Canical	2022-09-20	2	185	82,693.75	Accumulation detection	158
Porto da Cruz, Praia da Maiata	2022-09-15	1	30	20,317.19	ML mapping	321
		1	60	26,935.81	ML mapping	222
		1	60	26,935.81	ML mapping	221
Porto Santo, Porto dos Frades	2022-10-12	1	30	1,305.42	ML mapping	61
		1	60	1,095.19	ML mapping	54
Porto Santo, Serra de Dentro	2022-10-12	1	30	4,023.94	ML mapping	191

2.3. Accumulation Detection

Flight operations were manually conducted from land, on the north coast of Canical, to inspect the cliff shoreline (Figure 2), assess accumulation areas and direct clean-up efforts. Operations were coordinated with 3 vessels going to the area. Two consecutive flights were conducted: one to inspect cliffs and shoreline

and detect areas with visible marine debris accumulation, and; a second to collect imagery and do 3D digital model of the shoreline.

Take-off and landing was on top of the cliff and special attention was required to maintain connection and a direct line of sight to the UAS while inspecting the target area (> 10 ha). After detecting areas with highest visible marine debris accumulation, areas of highest visible accumulation of marine were reported (i.e. by phone) to DRAAC team on vessels to enable best clean-up effort allocation and optimisation.

Following inspection flight, a mapping flight was conducted manually, using a 10 second timer to collect imagery and following the shore line profile while maintaining 50% approximate overlap between subsequent images. A total of 157 images were collected during the manual mapping flight.

Collected images were sorted and uploaded Pix4D Cloud processing. Processing options included: multiscale, (Half of the image size), an optimal point density and a minimum of 3 matching points and a 3D Texture Mesh with medium resolution and no color balancing.

Aerial surveys used a DJI Mavic 2 ZOOM, a widely available quadcopter with a 1/2.3" CMOS with 12 million effective pixels and 83° of maximum field of view. Flight operations relied on DJI Groundstation iOS software installed in an iPad connected to a DJI MAVIC remote controller.

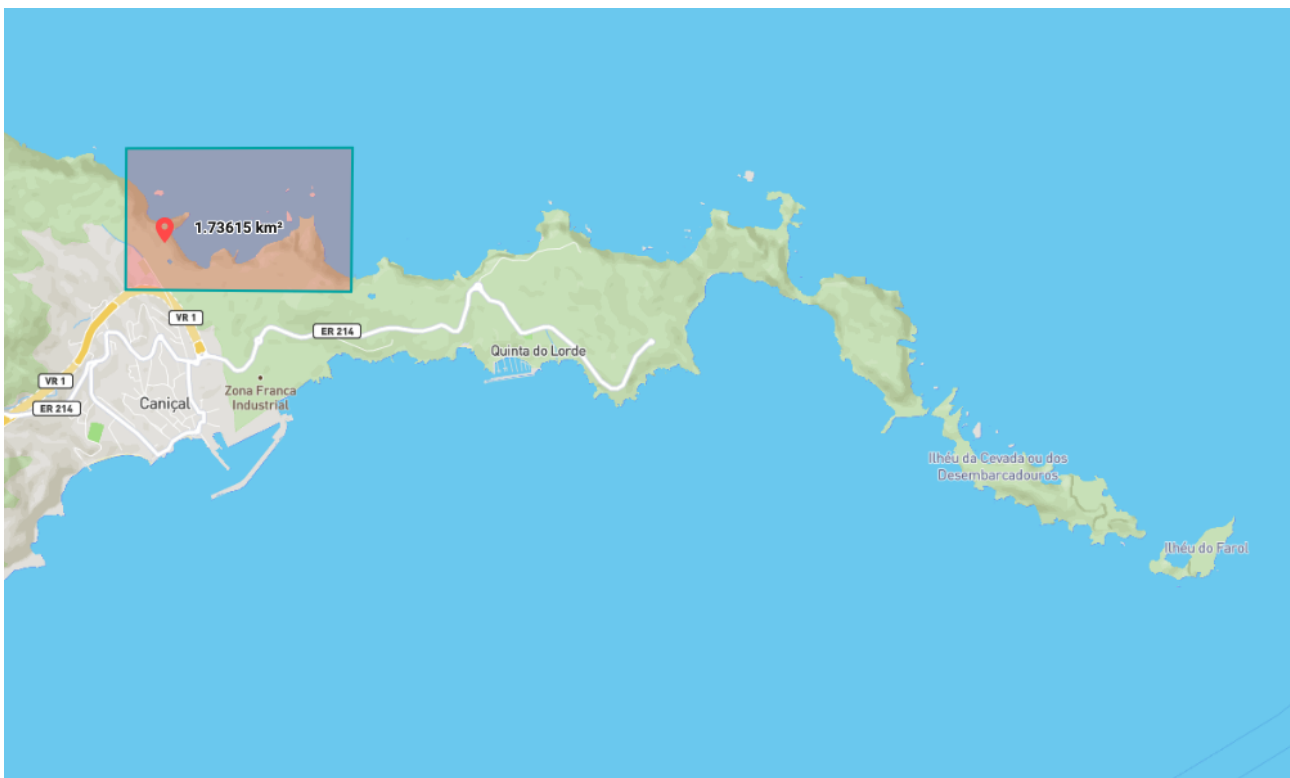


Figure 1. Map of shoreline area of interest for inspection and litter accumulation detection (shaded area) and of take-off and landing groundstation (marker).

2.4. Mapping beached litter concentration

Flight patterns and parameters were planned and conducted within DJI Groundstation 3d mapping interface. Flights ranged in altitude (30-100 m), covered area (1000-26,000 m²), location (4 OSPAR monitoring sites) and image overlap (60-70% side overlap and 70-90% front overlap). Aerial surveys used a DJI Mavic 2 PRO, a widely available quadcopter with a 1" CMOS with 20 million effective pixels and a 77° of field of view. Flight operations relied on DJI Groundstation iOS software installed in an iPad connected to a DJI MAVIC remote controller.

Collected images were sorted and uploaded to Pix4D Cloud for processing. Processing options included: multiscale, (half of the image size), an optimal point density and a minimum of 3 matching points and a 3D Texture Mesh with medium resolution and no color balancing.

Output mosaics and 3d texture mesh from flights at different altitudes were visually inspected in Pix4Dcloud web interface to assess feasibility to visually detect litter items and total area covered. In selected flights, identifiable litter items were annotated using two types of labels: *Litter item* and *Likely litter item* based on the confidence of the user. The use of these two confident levels is to enable the production of a minimum concentration map with higher confidence level and a higher concentration map with lower confidence level. Orthophotomosaics and annotations were then exported as GeoTIFF and shapefiles for use in a GIS software (e.g. ArcGIS PRO, QGIS).

In GIS software the total beach area and the OSPAR monitoring area was manually digitised and used for density estimates. Number of items identified *in situ* and the number of items detected inside the *in situ* survey area, by visually inspecting the imagery, were compared and used to estimate a correction factor (i.e. *in situ* counts were used as reference to calculate underestimation by visual inspection of imagery). Using the calculated correction factor, an extrapolation for the entire beach area was used to assess litter densities and concentrations in the entire beach. Results can be displayed as heatmaps to facilitate the identification of highest concentration of marine litter items within the surveyed area.

3. RESULTS

3.1. Accumulation Detection

Following the inspection and imagery collecting flights, the 157 images collected during the manual mapping mission were used to create a orthophotomosaic and 3D digital model of the target area where visible accumulation of marine debris had been detected on the video stream during the inspection flight (see Annex I: Processing Quality Report - Caniçal). The mosaic and 3D digital model can be explored and visually explored to revisit areas with marine debris accumulations (Figure 2). The visual inspection of 2D and 3D outputs enables the user to detect organic and inorganic debris in multiple areas of the shoreline.

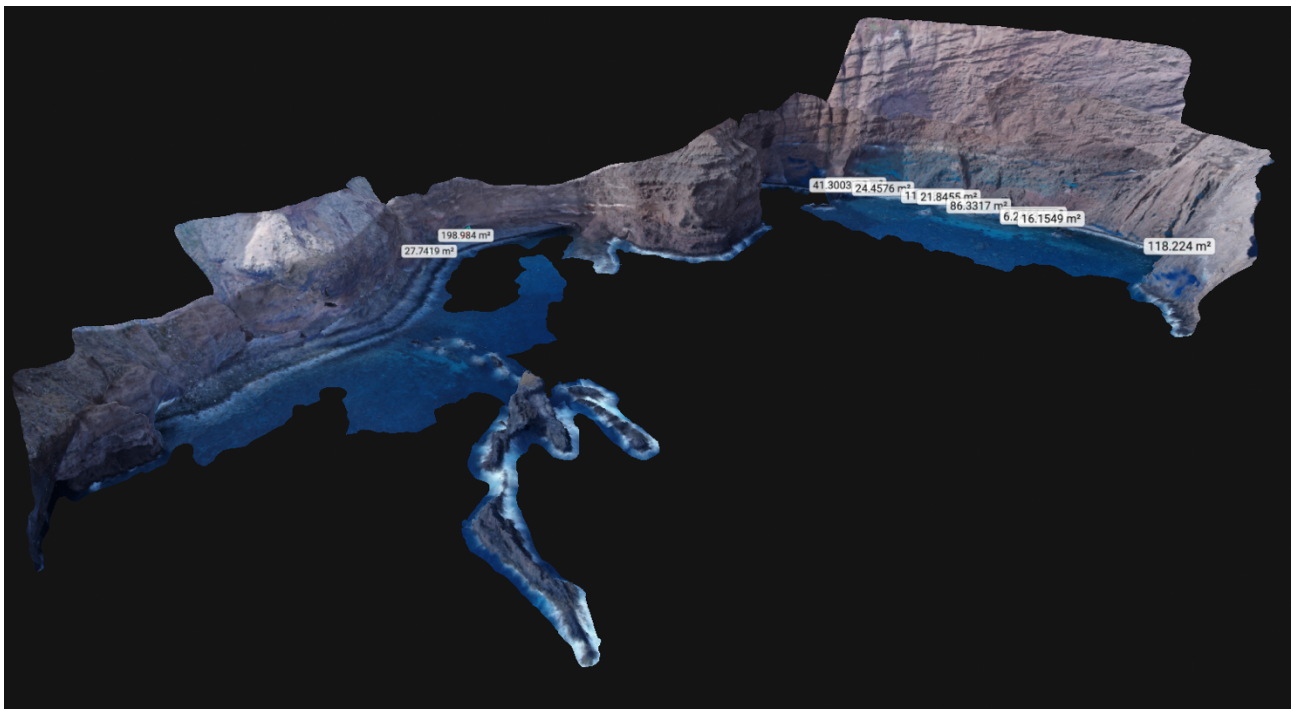


Figure 2. Three dimensional perspective of target area with accumualtion areas defined (click image to explore).

During this trial, three vessels were in the area with teams to conduct a clean-up. The pre-inspection of the target area allowed to collect information on the location and identify areas with higher visible concentrations of marine debris, which could be leveraged by clean up teams in the ground. Additionally, the inspection and analysis of images, orthophotomosaics and 3D textured mesh enables post analysis and follow up surveys.

3.2. Mapping beached litter concentration

The major objective of this pilot case study was to test and optimise a workflow that would integrate UAS remote sensing with existing beach litter monitoring programs and/or clean-up activities. We tested multiple altitudes and flight parameters to assess how these affect overall image resolution which determined by average (GSD) Ground Sampling Distance (2) which is calculated as:

$$GSD = \frac{H * s.width}{i.size * f.lenght}$$

where H is the flight altitude (m), $s.width$ is the sensor width (mm), $i.size$ is the size of image (pixels), and $f.lenght$ is the camera focal length (mm). Pix4D Cloud processing summaries provide average GSD for each flight.

Detection of small litter items (e.g. plastic bottle caps) require high resolution imagery with GSD between 0,5 and 1 cm (i.e. assuming you need at least 4 pixels to detect and recognise such small items). However, to achieve these resolutions using DJI Mavic 2 PRO, altitude must be set at 30 meters (producing an approximate average GSD of 0.77 cm). At this altitude, the approximate beach linear length covered is 300 m, increasing the area covered by in situ monitoring in 200%. There is compromise between resolution and spatial extent when optimizing the use of UAS based remote sensing to map litter pollution beyond the area monitored in situ. In the present case study, the goal was set increasing the are in more than 500% (a coastal extent of 500-600 meters). With goal set, optimal altitude was set at 60 meters, compromising resolution, and achieving mosaics with average GSDs between 1,6-2,0 cm.

Beach areas within mosaics were visually inspected and objects tagged with two litter item categories to map and estimate litter item density/concentration (Figure 3). In situ sampling provided characterization based on OSPAR categories (Figure 3-A) and subcategories Annex XXXX). The ratio between aerial counts and in situ counts inside the *in situ* monitoring area (Figure 3-A) were used to calibrate/correct litter estimates to the entire beach area (Figure 3-B).

Overall, the integration of UAS remote sensing with OSPAR in situ surveys provides: i) a detailed characterization of litter pollution, including which type of material and items are more common, ii) as assessment and map over a larger area, and iii) an overall estimate of litter density for the entire beach.

This information can be used for temporal analysis and identification of accumulation areas (Figure 4), which can be leveraged for mitigation actions and clean-ups.

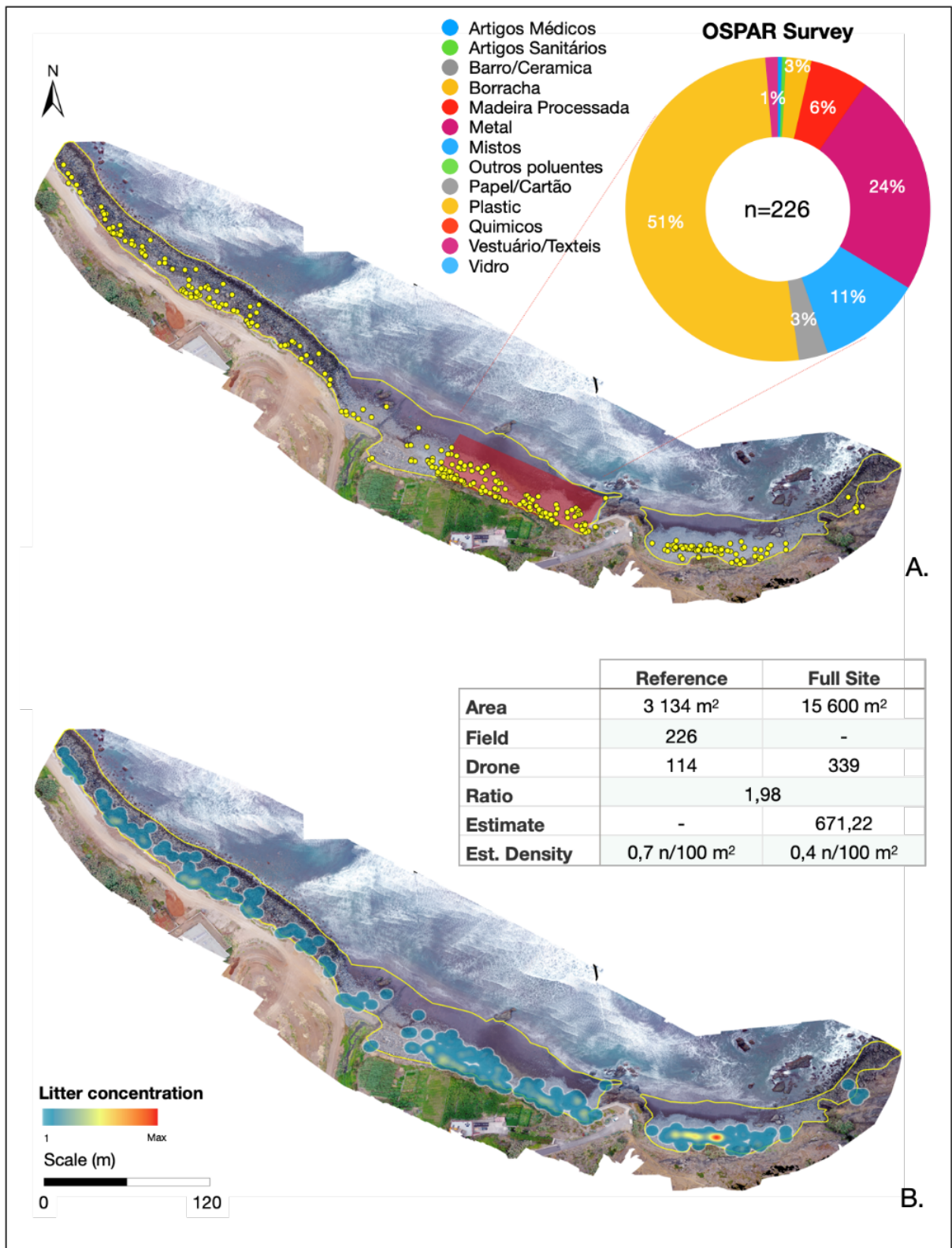


Figure 3. Orthophotomosaics of Praia da Maiata with: A. *in situ* sampling area (red shading) and material composition based on OSPAR category list (pie chart), litter items detected by image visual inspection (yellow dots) and total image inspection area (yellow line), and; B. Heatmap with litter item concentration based on image inspections with correction factor parameter table.

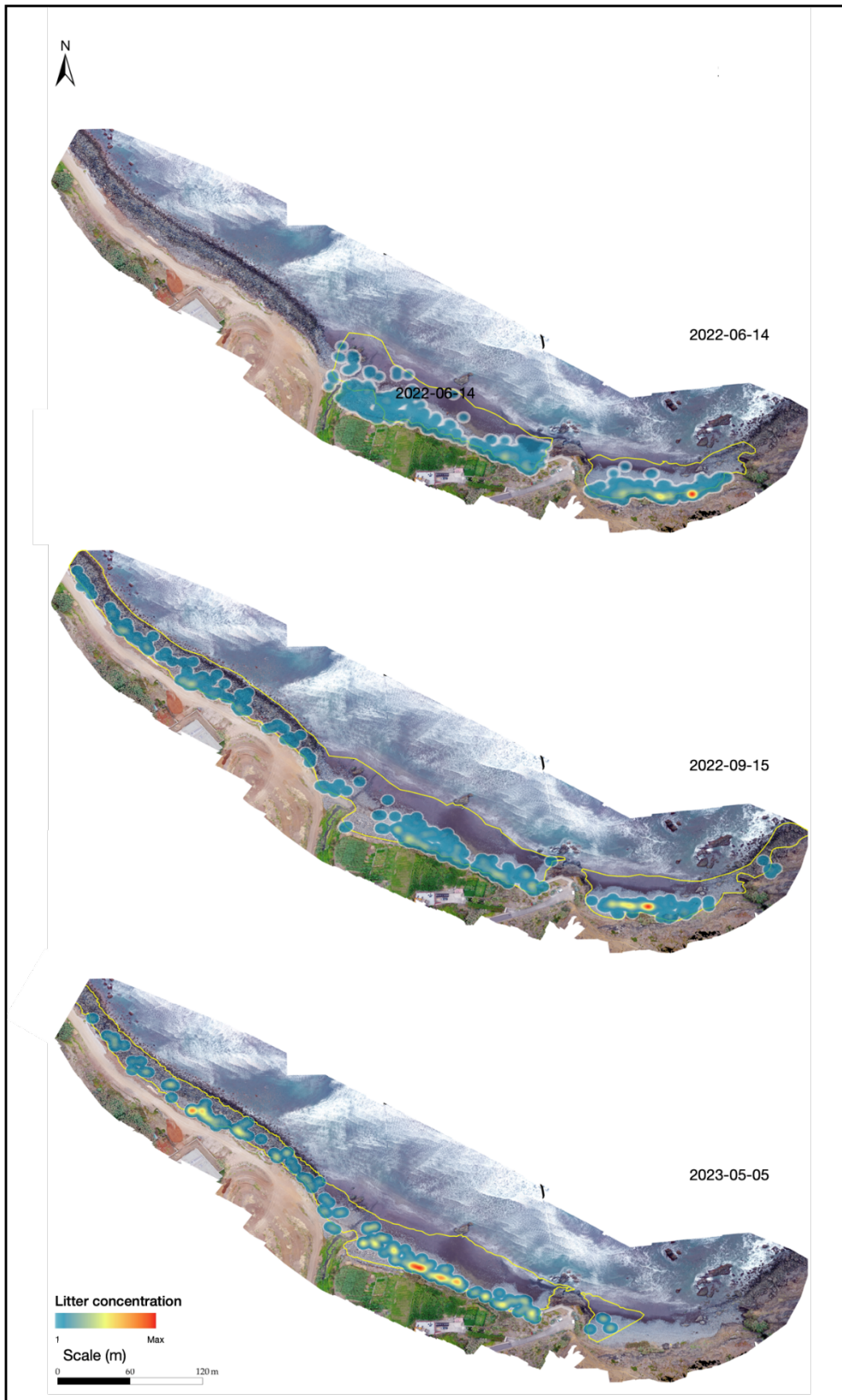


Figure 4. Orthophotomosaics of Praia da Maiata and heatmaps with litter item concentration based on image inspections (June 2022 on top, September 2022 in the middle and May 2023 on the bottom).

DISCUSSION

Leveraging UAS remote sensing for marine litter monitoring has been the focus of multiple studies, with research focusing on operational details and multiple imagery processing strategies and analytical approaches (1-6). Recent progress in the use of Artificial Intelligence and Deep Learning has effectively opened the way for automated image analysis and litter assessments (3-7). However, despite the promising future of AI assisted litter surveys using UAS remote sensing, these efforts are still not scalable to produce actionable outputs. Marine litter monitoring programs have two main objectives: i) characterize the type of litter so that mitigation and reduction policies and regulations can be targeted (e.g. straws, cigarette butts, plastic cutlery), and; ii) assess litter pollution over time and space. Actionable information regarding characterization data requires a high level of detail, enabling targeted actions for specific types of litter and sources. This level of detail required has shaped classification trees in EU guidelines and international litter monitoring programs (i.e. OSPAR and MSFD), to include a major category level that describes the type of material) and sub-category extensive list that details the item (8, 9).

In situ sampling and surveys provide accurate information addressing the first objective, which is to provide a detailed characterization of marine litter found on beaches, however, they do not provide detailed information on the distribution of litter on the surveyed area and the surveyed area is very small (100 meters of shoreline). UAS remote sensing can easily extend survey areas to include extensions of up to one km or more, however, to enable surveys of larger areas, detection of small items becomes impossible. Additionally, state of the art AI powered used for litter monitoring (4-7) still fall short on the ability to characterize litter items into the level of detailed required by EU or OSPAR (8, 9). Furthermore, analytical workflows leveraging state of the art AI assisted analysis require a high level of expertise to implement (1-7), making them hard to scale up and practically inaccessible for most organizations and teams responsible for beach litter monitoring. Despite the promising results of latest research, using UAS remote sensing and deep learning is still not to a level that can be leveraged for EU mandatory monitoring and reporting.

Notwithstanding the limitations described, UAS remote sensing can still be leveraged, especially if combined with *in situ* sampling. In this case study, we demonstrate two simple applications, where no high level of skills or computational infrastructure is required: i) the use of UAS remote sensing to inspect large target areas to detect visible accumulation areas, and ii) the use of UAS surveys, combined with *in situ* sampling to characterise litter pollution and provide spatially explicit data on litter concentration within a target area that extends beyond a sampling area. The latter can easily be implemented with: a recreational UAS with camera, a cloud based service to generate orthophotomosaics and label litter and GIS software. Training and skills requirements are equally simple: basic A1-A3 open UAS pilot license, basic understanding and training with structure from motion photogrammetry and basic familiarity with GIS.

With no prohibiting cost and simple to implement, this strategy can easily be scaled up and integrated into ongoing beach litter monitoring programs, where *in situ* sampling is complemented with survey flights followed by: i) automated mosaic generation; ii) image inspection and annotation (i.e. labelling litter items in image); iii) import image and labelled items as GIS layers; iv) estimate correction coefficient based on drone detected vs *in situ* detected ratio, and; v) produce spatially explicit data (e.g. litter concentration maps, corrected density estimates, litter item distribution). These outputs can be used for multiple purposes, ranging to better understanding coastal dynamics and identify areas where litter systematically accumulates to providing updated maps that can be used for clean-ups and litter pollution mitigation.

Despite effective, this strategy still requires laborious visual inspection of imagery to identify and label litter items, which should be perceived as an incentive for continued research into UAS sensing payloads (e.g. higher resolution cameras, multispectral and hyperspectral sensors), deep learning object detection and spectral analysis and collaborative online annotation tools and workflows to enhance UAS litter remote sensing and automate the analytical process.

4. CONCLUSION

Current research and efforts have been advancing UAS remote sensing and AI assisted workflows to detect and monitor beached litter. However, most of these advances are still far from real world applications as they do not meet the requirements of international monitoring programs or the level of detail required by the EU. As is, the level of litter characterization into categories and sub-categories can not be addressed by UAS remote sensing and AI. In this case study we provide insight on how UAS remote sensing can still be leveraged to detect accumulation areas (especially in remote locations where *in situ* surveys is impossible), to assess the distribution of litter items within target areas that go beyond sampling areas and to map litter concentration along the shoreline. We further showcase how to combine UAS surveys and in situ sampling to provide litter composition assessment, litter concentration maps and overall litter density estimates.

5. REFERENCES

1. Gil Gonçalves, Umberto Andriolo, Luísa M.S. Gonçalves, Paula Sobral, Filipa Bessa. 2022. Beach litter survey by drones: Mini-review and discussion of a potential standardization. *Environmental Pollution*. Volume 315 <https://doi.org/10.1016/j.envpol.2022.120370>
2. Almeida, Sílvia; Tomoya Kataoka; Diogo Martins; Paulo Aguiar; Radeta, Marko; Canning-Clode, João; Monteiro, Joao. "Designing UAS-based aerial survey monitoring programs to assess floating litter contamination". *Remote Sensing* 15(1):84 (2023). [10.3390/rs15010084](https://doi.org/10.3390/rs15010084)
3. Andriolo, U., Gonçalves, G., 2023. The octopus pot on the North Atlantic Iberian coast: A plague of plastic on beaches and dunes. *Mar. Pollut. Bull.* 192, 115099. <https://doi.org/10.1016/j.marpolbul.2023.115099>
4. Garcia-Garin, O., Monleón-Getino, T., López-Brosa, P., Borrell, A., Aguilar, A., Borja-Robalino, R., Cardona, L., Vighi, M., 2021. Automatic detection and quantification of floating marine macro-litter in aerial images: Introducing a novel deep learning approach connected to a web application in R. *Environ. Pollut.* 273. <https://doi.org/10.1016/j.envpol.2021.116490>
5. Papakonstantinou, A., Batsaris, M., Spondylidis, S., Topouzelis, K., 2021. A Citizen Science Unmanned Aerial System Data Acquisition Protocol and Deep Learning Techniques for the Automatic Detection and Mapping of Marine Litter Concentrations in the Coastal Zone.
6. Hidaka, M., Matsuoka, D., Sugiyama, D., Murakami, K., Kako, S., 2022. Pixel-level image classification for detecting beach litter using a deep learning approach. *Mar. Pollut. Bull.* <https://doi.org/10.1016/j.marpolbul.2022.113371>
7. Takaya, K., Shibata, A., Mizuno, Y., Ise, T., 2022. Unmanned aerial vehicles and deep learning for assessment of anthropogenic marine debris on beaches on an island in a semienclosed sea in Japan. *Environ. Res. Commun.* 4. <https://doi.org/10.1088/2515-7620/ac473b>
8. Fleet, D., Vlachogianni, T. and Hanke, G., A Joint List of Litter Categories for Marine Macrolitter Monitoring, EUR 30348 EN, Publications Office of the European Union, Luxembourg, 2021, ISBN 978-92-76-21445-8, doi:10.2760/127473, JRC121708.
9. Hanke G; Galgani F; Werner S; Oosterbaan L; Nilsson P; Fleet D; Kinsey S; Thompson R; Palatinus A; Van Franeker J; Vlachogianni T; Scoullou M; Veiga J; Matiddi M; Alcaro L; Maes T; Korpinen S; Budziak A; Leslie H; Gago J; Liebezeit G. Guidance on Monitoring of Marine Litter in European Seas . EUR 26113. Luxembourg (Luxembourg): Publications Office of the European Union; 2013. JRC83985

ANNEX I

Quality Report



Generated with Pix4Denterprise version 4.8.0
Preview



Important: Click on the different icons for:



Help to analyze the results in the Quality Report



Additional information about the sections



Click [here](#) for additional tips to analyze the Quality Report

Summary



Project	20220920
Processed	2022-09-22 15:48:43
Camera Model Name(s)	FC2204_4.4_4000x3000 (RGB), FC2204_8.6_4000x3000 (RGB), FC2204_4.5_4000x3000 (RGB), FC2204_7.9_4000x3000 (RGB)
Average Ground Sampling Distance (GSD)	5.85 cm / 2.30 in
Area Covered	0.327 km ² / 32.7214 ha / 0.13 sq. mi. / 80.8981 acres
Time for Initial Processing (without report)	07m:51s

Quality Check



Images	median of 38165 keypoints per image	
Dataset	147 out of 157 images calibrated (93%), 1 images disabled	
Camera Optimization	2.73% relative difference between initial and optimized internal camera parameters	
Matching	median of 10676 matches per calibrated image	
Georeferencing	yes, no 3D GCP	

Preview

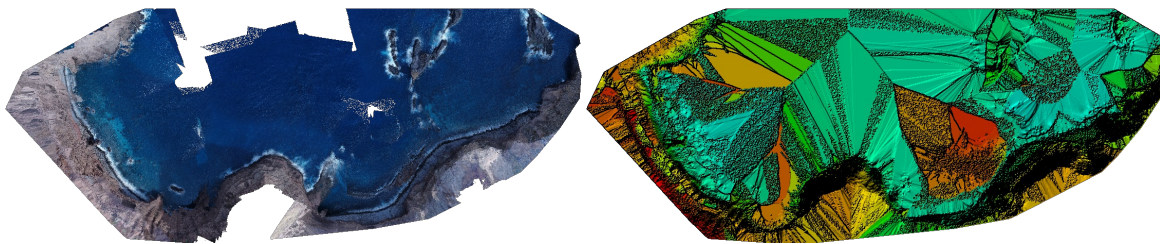


Figure 1: Orthomosaic and the corresponding sparse Digital Surface Model (DSM) before densification.

Calibration Details



Number of Calibrated Images	147 out of 158
Number of Geolocated Images	158 out of 158

Initial Image Positions



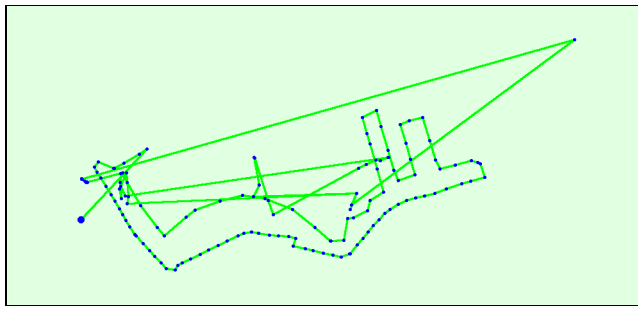
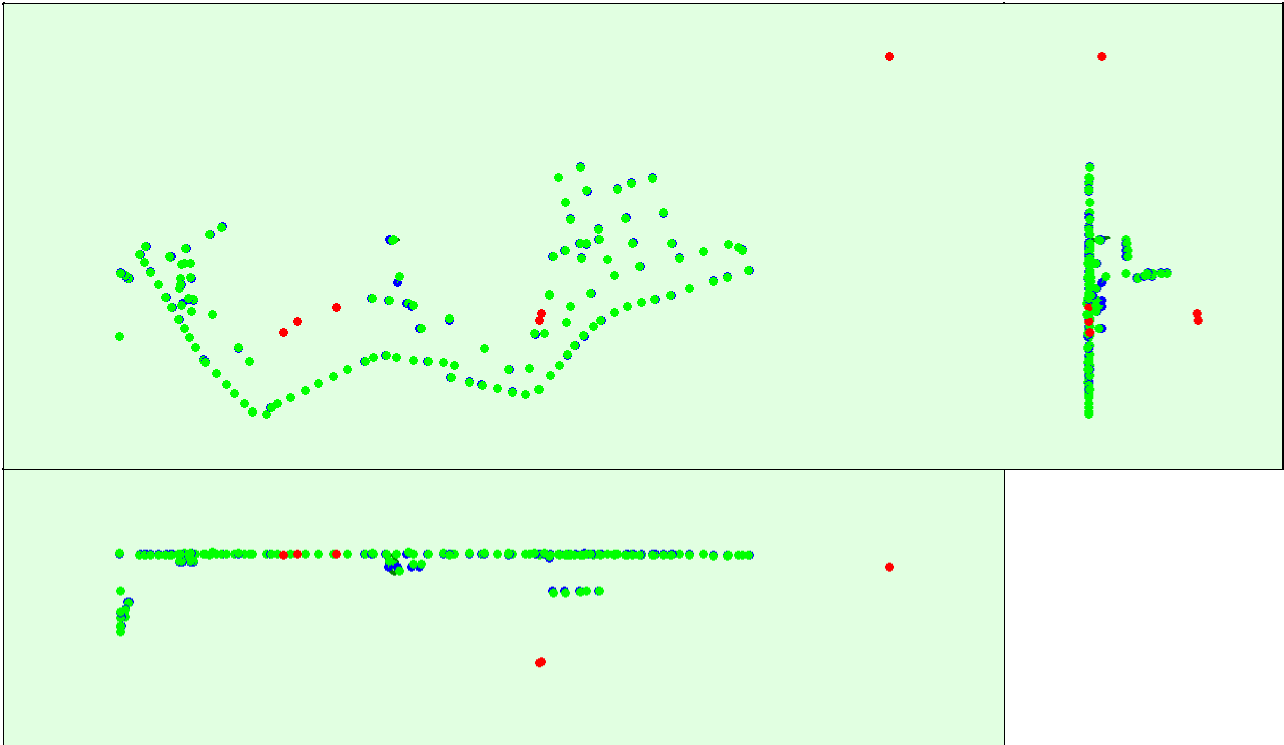


Figure 2: Top view of the initial image position. The green line follows the position of the images in time starting from the large blue dot.

Computed Image/GCPs/Manual Tie Points Positions



Uncertainty ellipses 50x magnified

Figure 3: Offset between initial (blue dots) and computed (green dots) image positions as well as the offset between the GCPs initial positions (blue crosses) and their computed positions (green crosses) in the top-view (XY plane), front-view (XZ plane), and side-view (YZ plane). Red dots indicate disabled or uncalibrated images. Dark green ellipses indicate the absolute position uncertainty of the bundle block adjustment result.

Absolute camera position and orientation uncertainties



	X [m]	Y [m]	Z [m]	Omega [degree]	Phi [degree]	Kappa [degree]
Mean	0.155	0.047	0.270	0.084	0.035	0.145
Sigma	0.001	0.001	0.001	0.018	0.009	0.024

Overlap

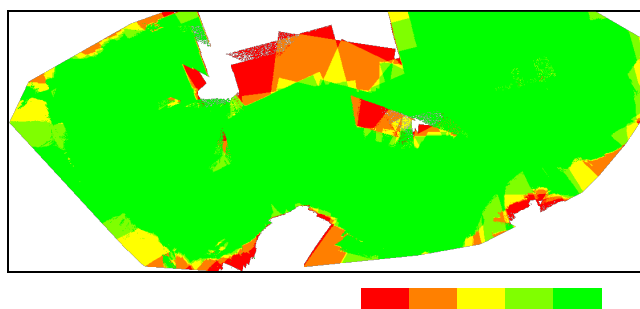


Figure 4: Number of overlapping images computed for each pixel of the orthomosaic.
 Red and yellow areas indicate low overlap for which poor results may be generated. Green areas indicate an overlap of over 5 images for every pixel. Good quality results will be generated as long as the number of keypoint matches is also sufficient for these areas (see Figure 5 for keypoint matches).

Bundle Block Adjustment Details

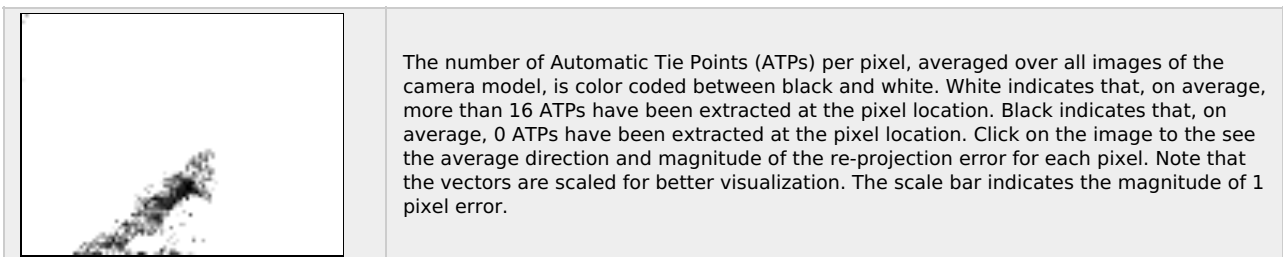
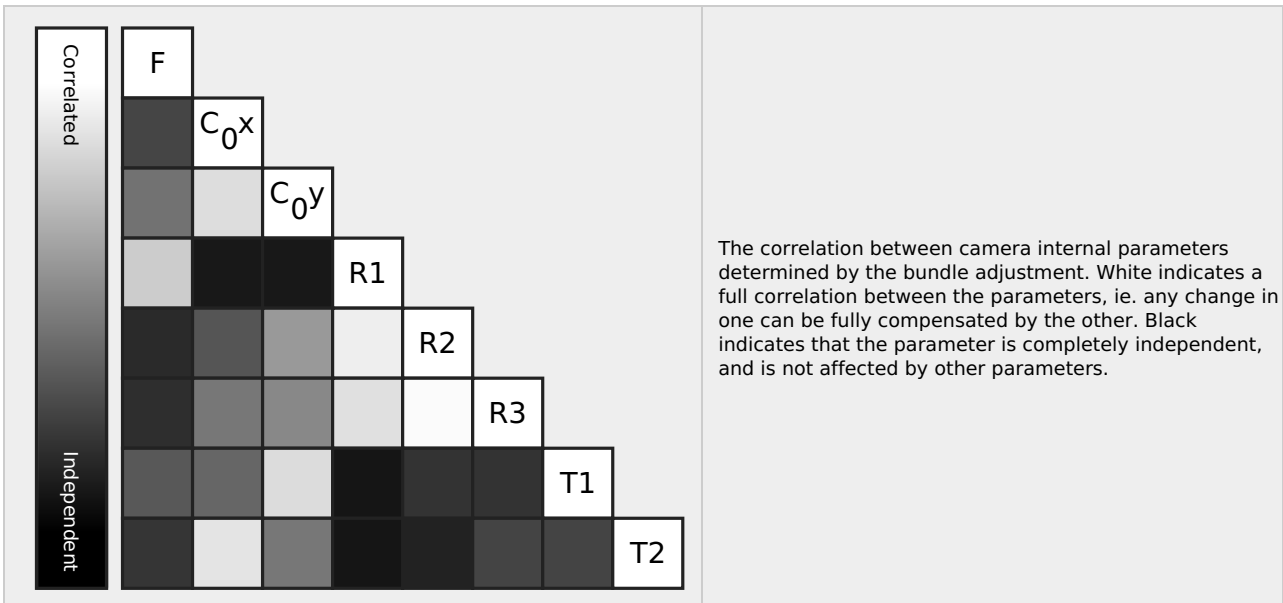
Number of 2D Keypoint Observations for Bundle Block Adjustment	1718597
Number of 3D Points for Bundle Block Adjustment	577396
Mean Reprojection Error [pixels]	0.174

Internal Camera Parameters

FC2204_4.4_4000x3000 (RGB). Sensor Dimensions: 6.396 [mm] x 4.797 [mm]

EXIF ID: FC2204_4.4_4000x3000

	Focal Length	Principal Point x	Principal Point y	R1	R2	R3	T1	T2
Initial Values	2742.856 [pixel] 4.386 [mm]	1999.999 [pixel] 3.198 [mm]	1500.000 [pixel] 2.399 [mm]	0.000	0.000	0.000	0.000	0.000
Optimized Values	2879.460 [pixel] 4.604 [mm]	1982.927 [pixel] 3.171 [mm]	1502.546 [pixel] 2.403 [mm]	-0.028	0.032	-0.023	-0.000	-0.002
Uncertainties (Sigma)	0.256 [pixel] 0.000 [mm]	0.203 [pixel] 0.000 [mm]	0.224 [pixel] 0.000 [mm]	0.000	0.000	0.000	0.000	0.000

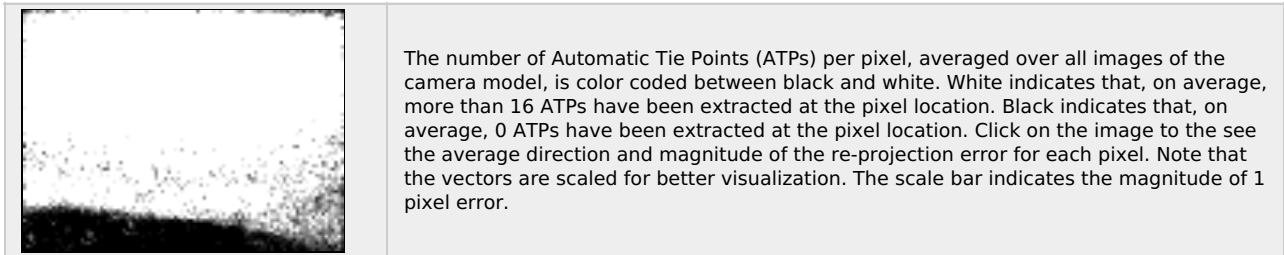
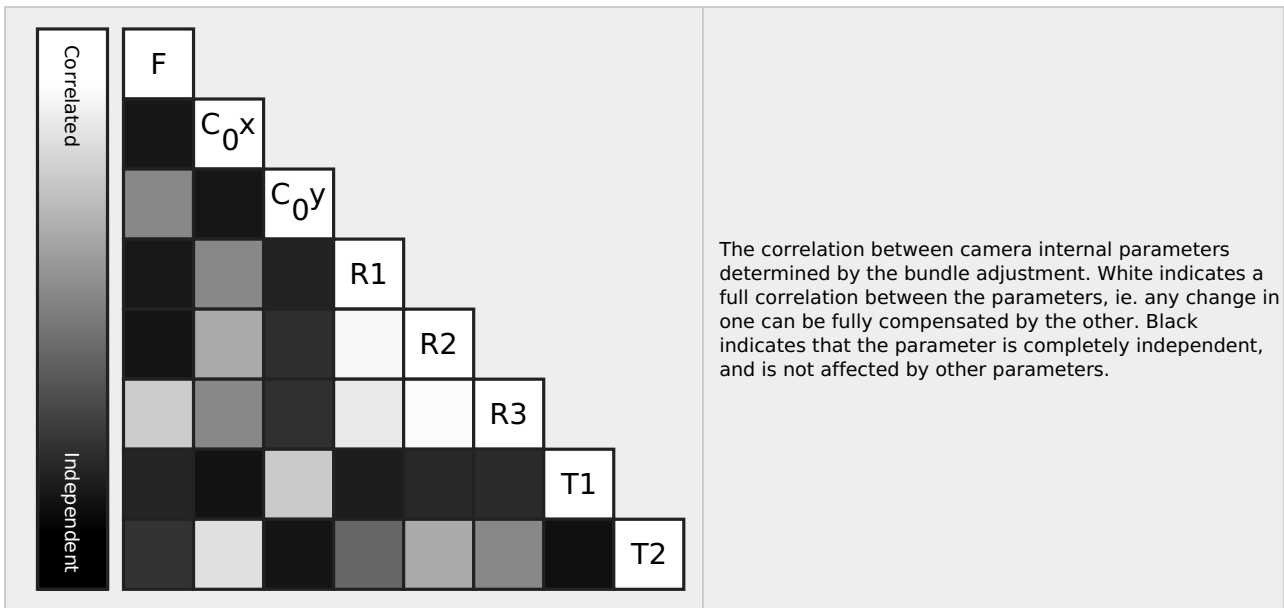


Internal Camera Parameters

FC2204_8.6_4000x3000 (RGB). Sensor Dimensions: 6.271 [mm] x 4.703 [mm]

EXIF ID: FC2204_8.6_4000x3000

	Focal Length	Principal Point x	Principal Point y	R1	R2	R3	T1	T2
Initial Values	5485.716 [pixel] 8.600 [mm]	2000.001 [pixel] 3.135 [mm]	1500.001 [pixel] 2.352 [mm]	0.000	0.000	0.000	0.000	0.000
Optimized Values	5652.590 [pixel] 8.862 [mm]	1966.207 [pixel] 3.082 [mm]	1507.274 [pixel] 2.363 [mm]	0.497	-4.291	11.138	0.000	-0.002
Uncertainties (Sigma)	0.871 [pixel] 0.001 [mm]	0.782 [pixel] 0.001 [mm]	0.945 [pixel] 0.001 [mm]	0.002	0.022	0.080	0.000	0.000



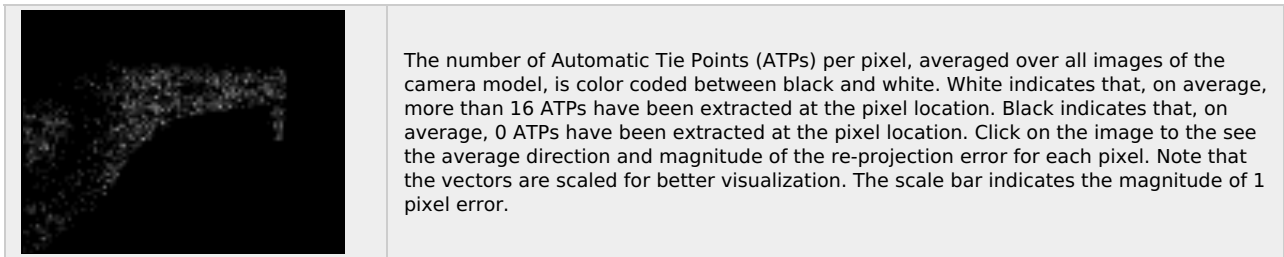
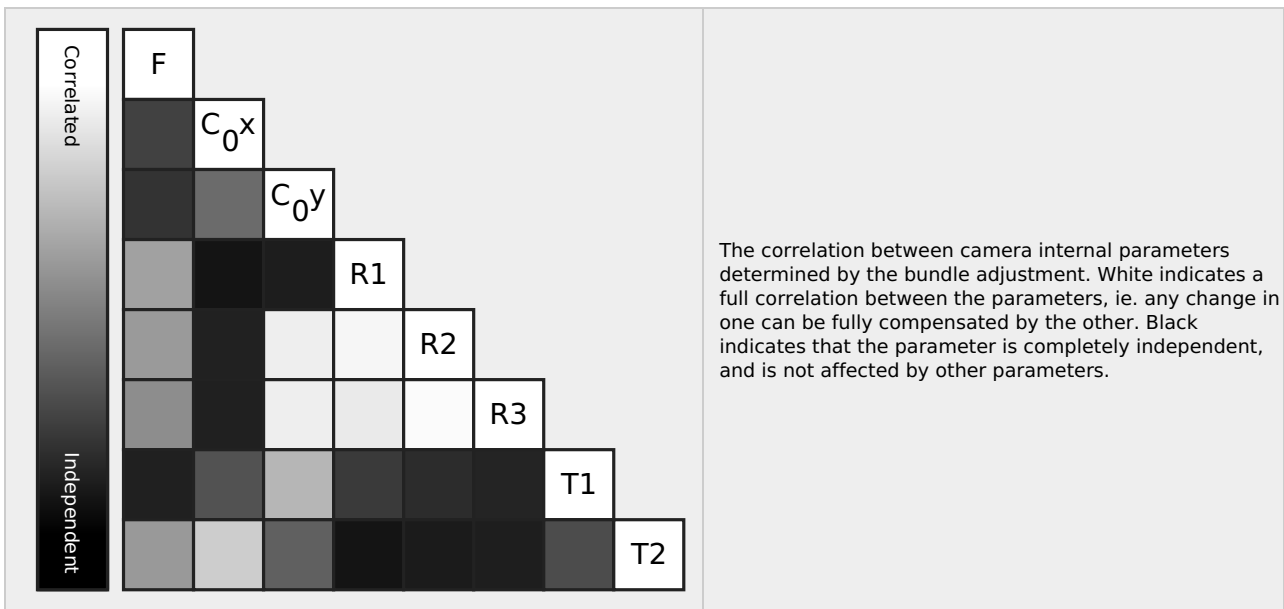
Internal Camera Parameters

FC2204_4.5_4000x3000 (RGB). Sensor Dimensions: 6.272 [mm] x 4.704 [mm]



EXIF ID: FC2204_4.5_4000x3000

	Focal Length	Principal Point x	Principal Point y	R1	R2	R3	T1	T2
Initial Values	2857.143 [pixel] 4.480 [mm]	2000.000 [pixel] 3.136 [mm]	1500.000 [pixel] 2.352 [mm]	0.000	0.000	0.000	0.000	0.000
Optimized Values	2939.732 [pixel] 4.610 [mm]	1982.741 [pixel] 3.109 [mm]	1499.706 [pixel] 2.352 [mm]	-0.026	0.033	-0.028	-0.000	-0.002
Uncertainties (Sigma)	1.098 [pixel] 0.002 [mm]	1.144 [pixel] 0.002 [mm]	1.018 [pixel] 0.002 [mm]	0.002	0.008	0.008	0.000	0.000



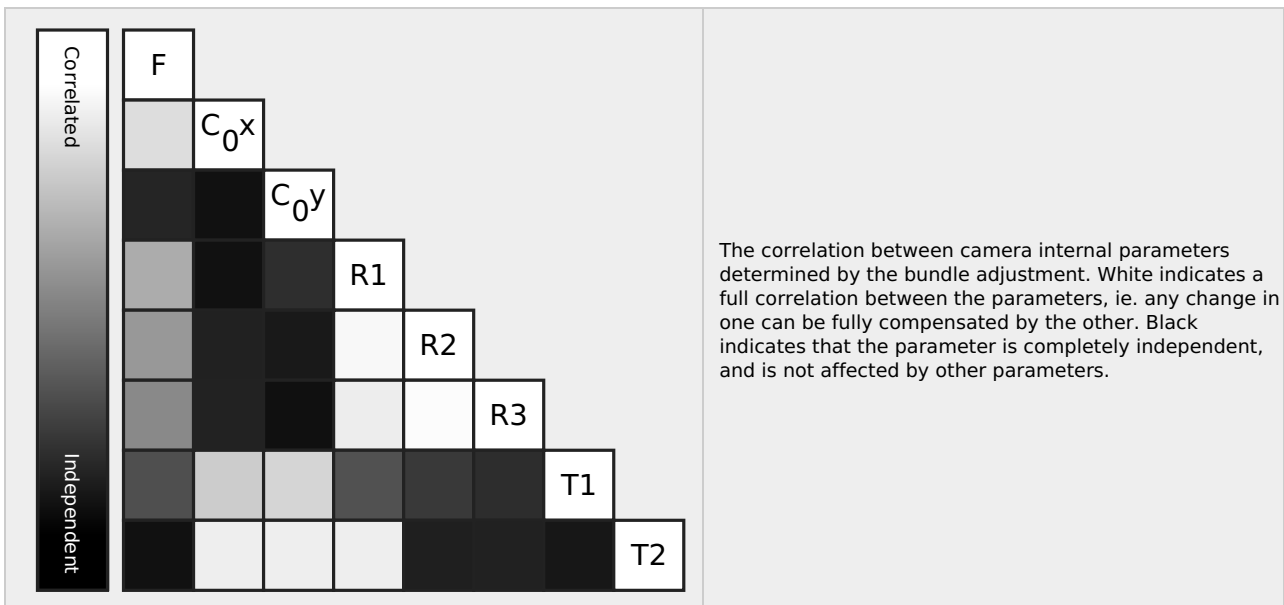
Internal Camera Parameters

FC2204_7.9_4000x3000 (RGB). Sensor Dimensions: 6.129 [mm] x 4.597 [mm]



EXIF ID: FC2204_7.9_4000x3000

	Focal Length	Principal Point x	Principal Point y	R1	R2	R3	T1	T2
Initial Values	5142.858 [pixel] 7.880 [mm]	2000.000 [pixel] 3.064 [mm]	1500.000 [pixel] 2.298 [mm]	0.000	0.000	0.000	0.000	0.000
Optimized Values	5143.668 [pixel] 7.881 [mm]	1981.578 [pixel] 3.036 [mm]	1503.130 [pixel] 2.303 [mm]	0.315	-2.250	4.852	0.000	-0.002
Uncertainties (Sigma)	3.021 [pixel] 0.005 [mm]	5.287 [pixel] 0.008 [mm]	3.690 [pixel] 0.006 [mm]	0.012	0.114	0.321	0.000	0.000





The number of Automatic Tie Points (ATPs) per pixel, averaged over all images of the camera model, is color coded between black and white. White indicates that, on average, more than 16 ATPs have been extracted at the pixel location. Black indicates that, on average, 0 ATPs have been extracted at the pixel location. Click on the image to see the average direction and magnitude of the re-projection error for each pixel. Note that the vectors are scaled for better visualization. The scale bar indicates the magnitude of 1 pixel error.

2D Keypoints Table



	Number of 2D Keypoints per Image	Number of Matched 2D Keypoints per Image
Median	38165	10676
Min	22177	330
Max	61687	35788
Mean	40971	11691

2D Keypoints Table for Camera FC2204_4.4_4000x3000 (RGB)

	Number of 2D Keypoints per Image	Number of Matched 2D Keypoints per Image
Median	35482	9173
Min	22177	330
Max	60559	32681
Mean	39538	10151

2D Keypoints Table for Camera FC2204_8.6_4000x3000 (RGB)

	Number of 2D Keypoints per Image	Number of Matched 2D Keypoints per Image
Median	47890	22620
Min	41564	10424
Max	61687	35788
Mean	51558	23116

2D Keypoints Table for Camera FC2204_4.5_4000x3000 (RGB)

	Number of 2D Keypoints per Image	Number of Matched 2D Keypoints per Image
Median	42728	0
Min	42728	14588
Max	42728	14588
Mean	42728	14588

2D Keypoints Table for Camera FC2204_7.9_4000x3000 (RGB)

	Number of 2D Keypoints per Image	Number of Matched 2D Keypoints per Image
Median	42683	0
Min	42683	11723
Max	42683	11723
Mean	42683	11723

Median / 75% / Maximal Number of Matches Between Camera Models

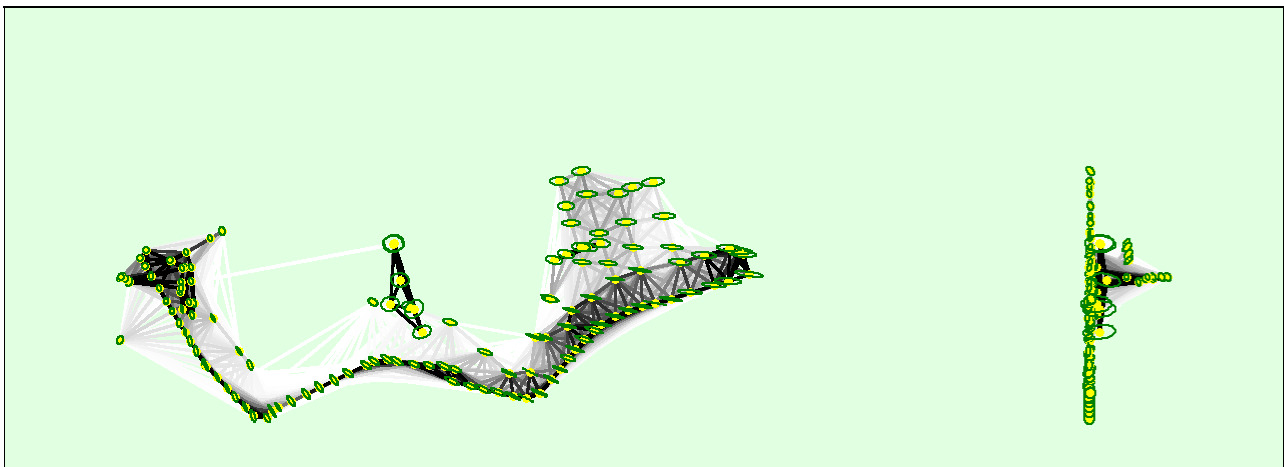
	FC2204_4.4_4000... (RGB)	FC2204_8.6_4000... (RGB)	FC2204_7.4_4000... (RGB)	FC2204_4.5_4000... (RGB)	FC2204_7.9_4000... (RGB)
FC2204_4.4_4000x3000 (RGB)	209 / 758 / 23904	688 / 1231 / 2910		1 / 1 / 12836	9 / 2601 / 2601
FC2204_8.6_4000x3000 (RGB)		7918 / 12962 / 22135		651 / 784 / 2091	358 / 9759 / 9759
FC2204_7.4_4000x3000 (RGB)					
FC2204_4.5_4000x3000 (RGB)					(n/a) / (n/a) / 2720

? 3D Points from 2D Keypoint Matches



	Number of 3D Points Observed
In 2 Images	340640
In 3 Images	111551
In 4 Images	54675
In 5 Images	29567
In 6 Images	13669
In 7 Images	8782
In 8 Images	5566
In 9 Images	3751
In 10 Images	2489
In 11 Images	1861
In 12 Images	1589
In 13 Images	1022
In 14 Images	637
In 15 Images	489
In 16 Images	340
In 17 Images	233
In 18 Images	162
In 19 Images	99
In 20 Images	66
In 21 Images	54
In 22 Images	38
In 23 Images	38
In 24 Images	31
In 25 Images	18
In 26 Images	8
In 27 Images	4
In 28 Images	6
In 29 Images	1
In 30 Images	2
In 31 Images	3
In 32 Images	2
In 33 Images	2
In 34 Images	1

? 2D Keypoint Matches





Uncertainty ellipses 100x magnified

Number of matches

25 222 444 666 888 1111 1333 1555 1777 2000

Figure 5: Computed image positions with links between matched images. The darkness of the links indicates the number of matched 2D keypoints between the images. Bright links indicate weak links and require manual tie points or more images. Dark green ellipses indicate the relative camera position uncertainty of the bundle block adjustment result.

Relative camera position and orientation uncertainties

	X [m]	Y [m]	Z [m]	Omega [degree]	Phi [degree]	Kappa [degree]
Mean	0.080	0.056	0.048	0.024	0.019	0.014
Sigma	0.046	0.015	0.034	0.014	0.004	0.014

Geolocation Details

Absolute Geolocation Variance

Min Error [m]	Max Error [m]	Geolocation Error X [%]	Geolocation Error Y [%]	Geolocation Error Z [%]
-	-15.00	0.00	0.00	0.00
-15.00	-12.00	0.00	0.00	0.00
-12.00	-9.00	0.00	0.00	0.00
-9.00	-6.00	0.00	0.68	0.68
-6.00	-3.00	1.36	0.68	1.36
-3.00	0.00	34.01	49.66	40.82
0.00	3.00	64.63	48.98	56.46
3.00	6.00	0.00	0.00	0.68
6.00	9.00	0.00	0.00	0.00
9.00	12.00	0.00	0.00	0.00
12.00	15.00	0.00	0.00	0.00
15.00	-	0.00	0.00	0.00
Mean [m]		0.026250	-0.037766	0.048243
Sigma [m]		0.798009	0.879311	1.403049
RMS Error [m]		0.798441	0.880122	1.403878

Min Error and Max Error represent geolocation error intervals between -1.5 and 1.5 times the maximum accuracy of all the images. Columns X, Y, Z show the percentage of images with geolocation errors within the predefined error intervals. The geolocation error is the difference between the initial and computed image positions. Note that the image geolocation errors do not correspond to the accuracy of the observed 3D points.

Relative Geolocation Variance

Relative Geolocation Error	Images X [%]	Images Y [%]	Images Z [%]
[-1.00, 1.00]	100.00	99.32	100.00
[-2.00, 2.00]	100.00	100.00	100.00
[-3.00, 3.00]	100.00	100.00	100.00

Mean of Geolocation Accuracy [m]	5.000000	5.000000	10.000000
Sigma of Geolocation Accuracy [m]	0.000000	0.000000	0.000000

Images X, Y, Z represent the percentage of images with a relative geolocation error in X, Y, Z.

Geolocation Orientational Variance	RMS [degree]
Omega	3.645
Phi	1.786
Kappa	5.556

Geolocation RMS error of the orientation angles given by the difference between the initial and computed image orientation angles.

Initial Processing Details

System Information

Hardware	CPU: Intel(R) Xeon(R) Platinum 8124M CPU @ 3.00GHz RAM: 69GB GPU: no info (Driver: unknown)
Operating System	Linux 5.15.0-1019-aws x86_64

Coordinate Systems

Image Coordinate System	WGS 84 (EGM 96 Geoid)
Output Coordinate System	WGS 84 / UTM zone 28N (EGM 96 Geoid)

Processing Options

Detected Template	 cloud-3d-maps-1*
Keypoints Image Scale	Full, Image Scale: 1
Advanced: Matching Image Pairs	Aerial Grid or Corridor
Advanced: Matching Strategy	Use Geometrically Verified Matching: no
Advanced: Keypoint Extraction	Targeted Number of Keypoints: Automatic
Advanced: Calibration	Calibration Method: Standard Internal Parameters Optimization: All External Parameters Optimization: All Rematch: Auto, yes

Point Cloud Densification details

Processing Options

Image Scale	multiscale, 1/2 (Half image size, Default)
Point Density	Optimal
Minimum Number of Matches	3
3D Textured Mesh Generation	yes
3D Textured Mesh Settings:	Resolution: Medium Resolution (default) Color Balancing: no
LOD	Generated: no
Advanced: 3D Textured Mesh Settings	Sample Density Divider: 1
Advanced: Image Groups	group1
Advanced: Use Processing Area	yes
Advanced: Use Annotations	yes
Time for Point Cloud Densification	02m:19s
Time for Point Cloud Classification	NA

Time for 3D Textured Mesh Generation	02m:42s
--------------------------------------	---------

Results



Number of Generated Tiles	1
Number of 3D Densified Points	6180944
Average Density (per m ³)	15.56

DSM, Orthomosaic and Index Details



Processing Options



DSM and Orthomosaic Resolution	1 x GSD (5.85 [cm/pixel])
DSM Filters	Noise Filtering: yes Surface Smoothing: yes, Type: Sharp
Raster DSM	Generated: yes Method: Inverse Distance Weighting Merge Tiles: yes
Orthomosaic	Generated: yes Merge Tiles: yes GeoTIFF Without Transparency: no Google Maps Tiles and KML: no
Time for DSM Generation	02m:46s
Time for Orthomosaic Generation	04m:31s
Time for DTM Generation	00s
Time for Contour Lines Generation	00s
Time for Reflectance Map Generation	00s
Time for Index Map Generation	00s

ANNEX II

ID OSPAR	30
Tipo monitorização	Regular
Período OSPAR	Outono
Ano	2022
Praia	Maiata - Porto da Cruz
Data	16-Sep-22
Nº visita monitorização	7
Nº de Pessoas	6
(1) Embalagens múltiplas – 4/6 (6 argolas ligadas e outro tipo de embalagem para latas)	0
(2) Sacos de asas/algas (p. ex. compras) incluindo pedaços (se permitirem identificação do objeto de origem)	0
(3) Sacos plásticos finos (p. ex. sacos para congelados) incluindo pedaços (se permitirem identificação do objeto de origem)	3
(112) União de sacos plásticos (Ripa que fica depois de retirar todos os sacos)	1
(410) Garrafas e Recipientes de Bebidas < 0,5 L	0
(420) Garrafas e Recipientes de Bebidas > 0,5 L	1
(5) Garrafas e Recipientes: Limpeza	2
(610) Embalagens: Alimentos incluindo os de “fast food” – plástico, incluindo pedaços (se permitirem identificação do objeto de origem)	20
(620) Embalagens: Alimentos incluindo os de “fast food” – espuma de poliestireno (esferovite), incluindo pedaços (se permitirem identificação do objeto de origem)	1
(7) Embalagens: Cosméticos (p. ex., loções solares, champô, gel de banho, desodorizante)	4
(8) Garrafas, Recipientes e Bidões: Óleo de motores (< 50 cm)	6
(9) Bidões: Óleo de motores (> 50 cm)	0
(10) “Jerry cans” (recipientes quadrados com pegas)	0
(11) Cartuchos de silicone	0
(12) Garrafas, Recipientes e Bidões: Outros	7
(13) Grades/Caixotes/Cestos: p. ex. Pão	1
(14) Partes de carro	2
(15) Cápsulas/tampas/argolas de cápsulas incluindo pedaços (se permitirem identificação do objeto de origem)	55
(16) Isqueiros	4
(17) Canetas e Tampas	0
(18) Pentas/escovas de cabelo/óculos	1
(191) Sacos de batatas fritas/guloseimas incluindo pedaços (se permitirem identificação do objeto de origem)	2
(192) Paus de chupa-chupa/gelados incluindo pedaços (se permitirem identificação do objeto de origem)	0
(20) Brinquedos e artigos recreativos ou de desporto tipicamente usados na praia (p. ex., pás, papagaios, bolas, etc.)	1
(211) Copo/chávena - plástico	2
(212) Copo/chávena – espuma de poliestireno (esferovite), incluindo pedaços (se permitirem identificação do objeto de origem)	0
(221) Pratos/Talheres/tabuleiros incluindo pedaços (se permitirem identificação do objeto de origem)	0
(222) Palhinhas e Misturadores/agitadores incluindo embalagem e pedaços (se permitirem identificação do objeto de origem)	2
(23) Sacos de fertilizantes/sacos de comida para animais	0
(24) Sacos de rede para vegetais, frutas e outros produtos	1
(25) Luvas (típicas de uso doméstico)	0
(113) Luvas (de uso industrial/profissional)	0
(26) Armadilhas para caranguejos/lagostas	0
(114) Etiquetas plásticas de uso em pesca e aquacultura	0
(27) Armadilhas para polvos / alcatruzes / covos	0
(28) Redes para ostras e sacos para mexilhão incluindo estacas	0
(29) Tabuleiros redondos para ostras (de culturas)	0
(30) Bandas de plástico para cultura de mexilhão (Tahitianas)	0
(31) Cordas /Cabos (diâmetro > 1 cm) incluindo pedaços (se permitirem identificação do objeto de origem)	3
(321) Cordas/cordéis (diâmetro < 1 cm) (indiferenciados) incluindo pedaços (se permitirem identificação do objeto de origem)	7
(322) Cordas/cordéis (diâmetro < 1 cm) de redes “manta de leão/funda do lobo” / “dolly ropes”	0
(115) Redes e peças de redes < 50 cm	6
(116) Redes e peças de redes > 50 cm	0
(331) Emaranhado de redes/cordéis (indiferenciados)	0
(332) Emaranhados de redes/cordéis “manta de leão/funda do lobo” / “dolly ropes”	0
(341) Caixas de pesca – plástico incluindo pedaços (se permitirem identificação do objeto de origem)	7
(342) Caixas de pesca - espuma de poliestireno (esferovite), incluindo pedaços (se permitirem identificação do objeto de origem)	0
(35) Linha de pesca (pesca com anzol)	0
(36) Tubos luminosos (tubos com líquido) incluindo embalagem	1
(37) Flutuadores e Boias para redes incluindo pedaços (se permitirem identificação do objeto de origem)	0
(38) Baldes incluindo pedaços (se permitirem identificação do objeto de origem)	5
(39) Tiras/cintas de embalagem incluindo pedaços	5
(40) Embalagens industriais/tiras de plástico, incluindo pedaços	0
(41) Fibra de vidro	0
(42) Capacetes de proteção	0
(43) Cartuchos de munições	4
(44) Sapatos/sandálias/chinelos e respetivos fragmentos	5
(45) Esponja de espuma (origem industrial, invólucros p. ex. garrafas, etc.)	59
(121) Sacos com fezes de cão	0
(1171) Fragmentos de plástico 0-2,5 cm	46
(461) Fragmentos de plástico 2,5 cm <= 50 cm	94
(471) Fragmentos de plástico > 50 cm	0
(1172) Fragmentos de espuma de poliestireno (esferovite) 0-2,5 cm	69
(462) Fragmentos de espuma de poliestireno (esferovite) 2,5 > 50 cm	50
(472) Fragmentos de espuma de poliestireno (esferovite) > 50 cm	0
(64) Beatas e Filtros de cigarro	1
(481) Meio suporte para biofilme (p. ex.: ETAR)	0
(48) Outros artigos de plástico/poliestireno (especificar na caixa de “outros”)	17
(482) Resíduos de construção (p. ex. canos, tubos, mangueira, etc.)	6
(483) Fechos para saco plástico e atilhos vários (p. ex. para etiquetas)	0
(484) Molus da Roupa	2
(485) Rótulos e Etiquetas várias	1
(486) Vasos de flores/pratos de vasos e fragmentos	17
(487) Iscos artificiais/amostras para pesca à linha	0
TOTAL PLÁSTICO	521
TOTAL PLÁSTICOS OSPAR (Macroplásticos)	406
(49) Balões (além disso as válvulas, fitas, haste suporte e cordéis, etc.), incluindo pedaços (se permitirem identificação do objeto de origem)	0
(50) Botas	0
(52) Pneus	0
(53) Outras peças de borracha (especificar na caixa de “outros”)	6
BORRACHA	6

(54) Roupas e fragmentos (p. ex. vestuário, toalhas, bonés, etc.)	1
(55) Artigos de casa (p. ex. carpetes, cortinados, etc.)	0
(551) Fitas, atilhos, cordão, laços, e outros adornos, etc.	0
(56) Sacos e mochilas (couro e tecido) incluindo pedaços (se permitirem identificação do objeto de origem)	0
(57) Calçado (couro e tecido) incluindo pedaços (p. ex. sapatos/sandálias, etc.)	2
(59) Outros têxteis (especificar na caixa de "outros")	0
VESTUÁRIO/TÊXTEIS	3
(60) Sacos	2
(61) Cartão (p. ex. caixas, incluindo pedaços)	0
(118) Caixas/Tetrapacks para leite	0
(62) Outros Tetrapacks (p. ex. sumo, vinho, etc.)	0
(63) Pacotes de cigarros incluindo a película exterior e folha interior	0
(65) Copos, incluindo pedaços	0
(66) Jornais/ Revistas, incluindo pedaços	1
(67) Outras peças de papel/cartão (especificar na caixa "outros")	5
(671) Raspadinhas, Euromilhões e semelhantes	0
(672) Guardanapos, lenços de papel, papel higiénico e fragmentos	2
PAPEL /CARTÃO	10
(68) Rolha (cortiça)	0
(69) Paletes incluindo pedaços (se permitirem identificação do objeto de origem)	0
(70) Grades/caixotes incluindo pedaços (se permitirem identificação do objeto de origem)	0
(71) Armadilhas para caranguejos/lagostas	0
(119) Caixas de peixe incluindo pedaços (se permitirem identificação do objeto de origem)	0
(72) Paus de gelados e outros utensílios para alimentos	0
(73) Trinchas de pintura	0
(74) Outras madeiras ou pedaços < 50 cm (especificar na caixa de "outros")	14
(75) Outras madeiras ou pedaços > 50 cm (especificar na caixa de "outros")	0
MADEIRA PROCESSADA	14
(76) Aerosóis/latas de spray	1
(77) Tampas (caricas)/coberturas/fecho "abertura fácil"	0
(78) Latas de bebidas incluindo pedaços (se permitirem identificação do objeto)	0
(120) Grelhas de um só uso	0
(79) Pequenos eletrodomésticos e outros dispositivos elétricos	0
(80) Artigos para pesca incluindo pedaços (Chumbos/pesos)	0
(81) Folha metálica (p. ex. alumínio)	0
(82) Lata de comida incluindo pedaços (se permitirem identificação do objeto de origem)	0
(83) Escórias industriais	0
(84) Bidões de óleo	0
(86) Latas/Tinas de tinta	0
(87) Armadilhas para caranguejos/lagostas	0
(88) Arame, rolo de arame, arame farpado	1
(89) Outras peças de metal < 50 cm (especificar na caixa de "outros")	27
(891) Ferros para construção civil	24
(90) Outras peças de metal > 50 cm (especificar na caixa de "outros")	2
METAL	55
(91) Garrafas incluindo pedaços (se permitirem identificação do objeto de origem)	1
(92) Lâmpadas redondas/tubulares	0
(931) Frascos de vidro (p. ex. frascos de compota, conserva, etc.)	0
(932) Frascos de pesticidas e outros químicos	0
(93) Outras peças de vidro (especificar na caixa de "outros")	0
VIDRO	1
(94) Material de construção (p. ex. azulejo, telha, tijolos, etc.)	19
(95) Alcatruzes para polvos/covos	0
(96) Outras peças de cerâmica/construção (especificar na caixa de "outros")	0
BARRO/CERÂMICA	19
(97) Preservativos incluindo embalagem - plástico	0
(981) Cotonetes - bastonete de plástico	0
(982) Cotonetes - bastonete de cartão	0
(99) Toalhetes de limpeza/fraldas/pensos - plástico	0
(100) Tampões e aplicadores de tampões incluindo invólucros - plástico	0
(101) Ambientadores sanitários (WC/toilet fresheners) - plástico	0
(1021) Toalhetas húmidas/wet wipes - plástico	0
(1022) Escova de dentes/fio dentário/escovilhão - plástico	1
(102) Outros artigos sanitários (especificar na caixa de "outros")	0
ARTIGOS SANITÁRIOS	1
(103) Recipientes/tubos/carteiras/blister (médicos e farmacêuticos)	1
(104) Seringas e tampas de agulha	0
(105-1) Máscaras faciais de uso único - plástico	0
(105-2) Luvas de uso único - plástico	0
(105) Outros artigos médicos (mechas de algodão, ligaduras, pensos rápidos, etc.) (especificar na caixa de "outros")	1
(105-3) Viseiras	0
(105-4) Embalagens alcool/gel desinfetante	0
ARTIGOS MÉDICOS	2
(150) Cápsulas de Café	1
(151) Fios elétricos, esticadores, etc.	21
(152) Outros artigos mistos (especificar na caixa de "outros")	3
(153) Conglomerados - construção civil	0
MISTOS	25
(108) Gama de tamanho 0-1cm	0
(109) Gama de tamanho 1-10 cm	0
(110) Gama de tamanho >10 cm	0
QUÍMICOS FLUTUANTES	0
VISCOSOS e PERSISTENTES (p. ex. parafinas) (nº de unidades por metro de linha de costa)	
VISCOSOS e PERSISTENTES (p. ex. parafinas)	
111 (Outros poluentes)	0
OUTROS POLUENTES (ex: alcatrão)	0
Objetos/100m (Macrolixo)	542
Pellets	Sim
Carvão	Não
PESO (Kg)	50,5
Total (contando com meso e micro)	657